International Journal of Applied Power Engineering (IJAPE)
Vol. 15, No. 3, September 2026, pp. 1422~1438
ISSN: 2252-8792, DOI: 10.11591/ijape.v15.i3.pp1422-1438

Comparative study of MPPT algorithm on photovoltaic string under partial shading

Dikpride Despa[1,2], Gigih Forda Nama[3,4], Zulmiftahul Huda[1], Stefanus Debiarto Marudut Sagala[1]
[1]Department of Electrical Engineering, University of Lampung, Bandar Lampung, Indonesia
[2]Engineer Professional Programme Study Programme, University of Lampung, Bandar Lampung, Indonesia
[3]Department of Informatics, University of Lampung, Bandar Lampung, Indonesia
[4]Doctoral Program of Environmental Science, University of Lampung, Bandar Lampung, Indonesia

Article Info

Article history:

Received Sep 4, 2025
Revised Jul 1, 2026
Accepted Aug 15, 2026

Keywords:

Flower pollination algorithm
Metaheuristic optimization
MPPT
Partial shading
Particle swarm optimization
Photovoltaic systems

ABSTRACT

Partial shading significantly degrades the photovoltaic (PV) performance value by introducing multiple peaks in power voltage (P-V) curve, complicating maximum power point tracking (MPPT). This research aims to presents a systematic comparative study of 4 MPPT algorithms, that are i) perturb and observe (P&O), ii) incremental conductance (InC), iii) particle swarm optimization (PSO), and iv) flower pollination algorithm (FPA), under 6 systematically testbeds modeled irradiance scenarios. The evaluation focused on tracking accuracy, convergence speed, and also robustness against local maxima entrapment. The findings indicated that slope-based algorithms (P&O and InC algorithm) achieved rapid convergence (<0.05 second), under uniform conditions but consistently fail to locate the global maximum power point (GMPP) in multi peak profiles, with efficiency dropping to ~83.6%. While the PSO algorithm succeeds in moderately faced complex cases, it fails under highly multimodal landscapes due to premature convergence. In contrast, for FPA algorithm consistently identifies the GMPP across all scenarios, its achieving superior tracking efficiency of up to 99.8%, despite requiring longer settling times (0.75-1.03 seconds) and exhibiting transient oscillations. These findings quantify the speed-accuracy trade-off in MPPT controllers and highlight the necessity of global optimization for reliable performance under dynamic shading. Future work will address the challenge of hardware implementation in the loop validation and computational efficiency for real-time embedded applications.

Corresponding Author:

Dikpride Despa
Department of Electrical Engineering, University of Lampung
Prof. Sumantri Borjonegoro Street, No.1 Gedong Meneng, Bandar Lampung, Indonesia
Email: despa@eng.unila.ac.id

1. INTRODUCTION

Solar energy adoption photovoltaic (PV), has become a key focus area in the global decarbonization agenda because of its ease of capacity extend process, competitive production costs, and no carbon emissions, make this technology critical. But solar panel performance is greatly influenced by how much sunlight it gets. Uneven irradiation (partial shading) occurs due to interference from the clouds, some dust or shades of surrounding objects. Under general light conditions, the P–V curve shows only a peak maximum power point (MPP), which is quite easy to control. However, when one part of the panel is obstructed, bypass diodes are activated, and a multimodal P–V curve (N curves) appears. This causes even greater complexity in the controlling process and a reduction of energy efficiency, but also exposes the module to localized overheating, provoking hot spots damage [1]-[3]. Thus, a strong maximum power point tracking (MPPT) mechanism is needed for the operation of PV systems in outdoor case.

The conventional MPPT algorithms based on the curve slope measurement, such as perturb and observe (P&O) [4] and incremental conductance (InC), are very popular because of their low computation burden and good response time under uniform irradiation condition [5]. But when it comes to multimodal P–V curves, the inherent weaknesses of these advanced algorithms come to light. The underlying logic makes the algorithms tend to lock onto local maximum power point (LMPP) as the first peak found is assumed to be the highest and take time to reach global maximum power point (GMPP) [6]. As a consequence, this limitation results in huge power losses since the GMPP is usually far from the search initial point [5], [7], [8].

To overcome this issue, metaheuristic based optimization methods have been increasingly utilized. Both of these algorithms are based on inertial based group movement and also social cognition, such as the particle swarm optimization (PSO) algorithm or utilize mechanisms like combinatorial Lévy flight based processes coupled with local pollination for solving complex landscape problems [9]-[11]. These are focused methods which have previously been shown as capable of accurately identifying GMPPs under partial shade conditions [12], [13]. Their direct applicability is limited by a strong dependence on parameter tuning, the sampling rate and also by power converter dynamics. Other limitations are there were long settling time need, transient oscillations, as well as an increased probability of premature convergence if diversity among the search population becomes too small [2], [14], [15].

While there have been many publications research on MPPT area, two major research gaps have been highlighted in several recent literature reviews. To illustrate, most comparative studies have only investigated a small range of shading conditions or less representative scenarios that do not closely resemble real-world conditions. Second, there is still no good standard for reporting on the dynamic performance indicators across a multi-peak curve testing such as convergence time, transient ripple, and resistance of local value traps. Moreover, experimental validation in hardware-in-the-loop (HIL) or outdoor testing is still limited when compared to proofs based solely on software simulations. Additionally, other operational aspects such as partial shadow detection and mechanisms to restart an attacked algorithm have not been comprehensively studied [2], [16]-[18].

Although other options of meta-heuristics are also possible for multimodal PV landscapes, such as genetic algorithms (GA) or grey wolf optimization (GWO), this work approaches a comparative analysis between PSO and flower pollination algorithm (FPA) (conventional methods). The reason to choose PSO and FPA is because they have respective benefits in preserving the pathways of global exploration and local exploitation effectively. FPA applies dynamic transition probabilities to alternate between global search and local exploitation, resulting in FPA being very adaptable for nonlinear optimization problem [19], [20]. Meanwhile, PSO is famous for its trajectory flexibility of particles in distinguishing local to global peaks [21]. The two methods have proven to be consistently more stable and competitive in searching the solution space given the characteristics of shadowed PV systems [22].

Hence, the objective of this manuscript is to show an extensive comparative study between P&O, InC, PSO and FPA for a total of six irradiation levels constrained to obtain up to five different crests in the P–V curve. This repeats for each scenario, such that the GMPP position varies wildly between starting at the first peak and finishing on the “edge” (the fifth peak). This method puts the LMPP-averse property of the algorithm under stringent scrutiny. Tests conducted on a PV string model attached to both a bypass diode and boost converter are then inspected via parameters, including tracking precision, convergence time length, and steady-state stability. This framework is intended to verify a testing measure of system accuracy, performance and dependability for outdoor uses [1]-[3], [23], [24].

This study makes three main contributions. The number one is the creation of a unified multi-scenario testbed, underpinning on the fifth peak scenario which was identified as the hardest part to search by any way. Second, it offers a deep synthesis of performance trade-offs: classical algorithms are fast but fail, while metaheuristics ensure (in theory) global search in exchange for extra time. Third, based on the testing data we provide a practical guide for system designers to choose among a multi of tested algorithms their single MPPT algorithm that is closer to the conditions they will be working with in the field, therefore helping them avoid complex hybrid approaches.

The structure of this article is as follows: Section 2 provides specifications about the PV system, converter and irradiation modeling design. Section 3 presents the comparative performance of the four algorithms, focusing on a review of accuracy and response time dynamics as well as an analysis of search failure when the peak point assumes the last position. Section 4 discusses a cross-scenario synthesis and practical implications for design of controllers. Lastly, Section 5 presents research findings and suggests future study, focusing on hardware-in-the-loop validation [2], sensitivity studies [15], and optimization of computational load imposed in embedded devices [25].

2. METHOD

2.1. Modeling of case scenarios

The PV system on this research consists of a five-module photovoltaic (PV) string connected in series, with each module equipped with bypass diodes to prevent reverse-bias stress and hot-spot formation under non-uniform irradiance [1], [3]. This configuration scenario was selected to generate a multi-peak power–voltage (P–V) curve and for enabling systematic evaluation of MPPT algorithms under partial shading conditions (Figure 1). The detail of technical specifications for each module is listed in Table 1. Bypass diodes implemented for providing an alternative current path when cells are shaded, reducing of power loss and for preventing the damage impact. Under normal conditions, these diodes remain reverse-biased; however, when shading occurs, they will become as forward-biased, act and allowing current to bypass shaded cells. This design to ensures realistic modeling of PV behavior under dynamic irradiance.

On this research, there were six irradiance testbed scenarios to emulate uniform and also partial shading conditions (Table 2). Scenario 1 represents uniform irradiance and producing a single peak, while on Scenarios 2–6 introduce the process of multiple peaks, with the GMPP migrating from the first to the fifth peak. This systematic variation will challenge all of algorithms that choose, for finding the ability to avoid local maxima and track the true GMPP, reflecting real-world shading patterns caused by clouds or obstructions [3], [16].

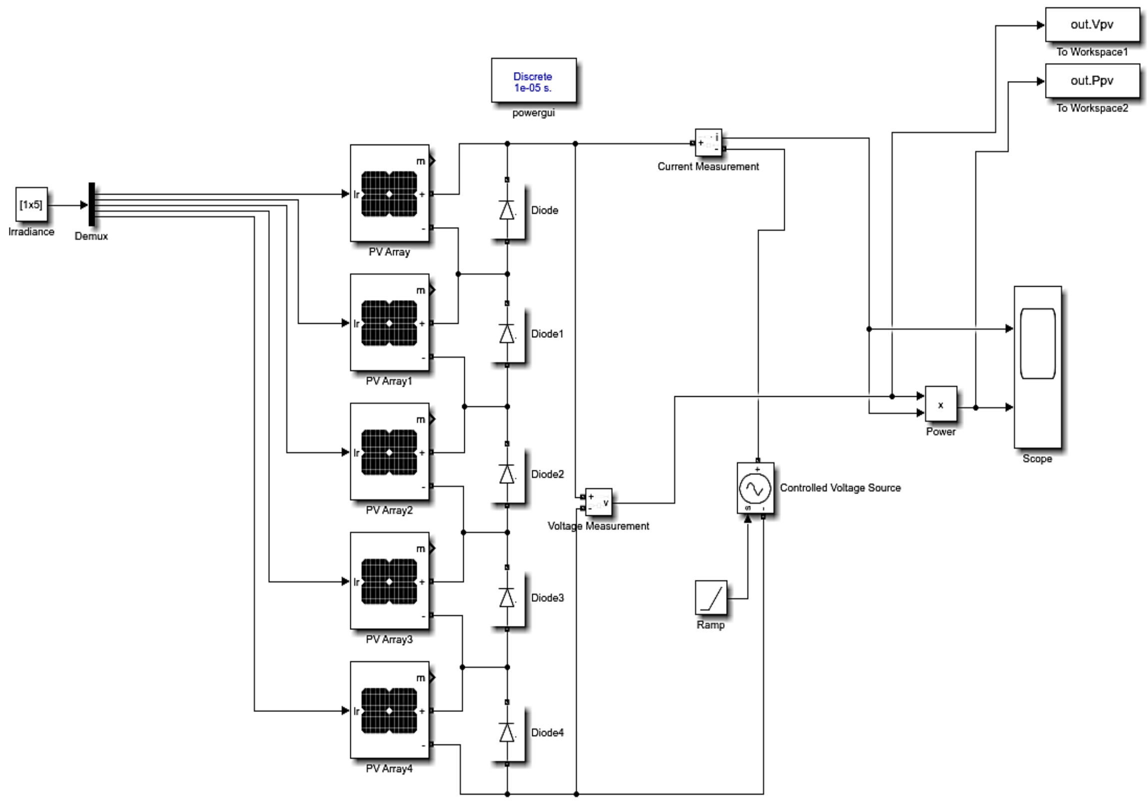

Figure 1. Modeled P–V characteristic curves for shading scenarios

Table 1. Photovoltaic specifications

Parameter	Value
Maximum power (p_{mpp})	600 Wp
Maximum voltage (v_{mpp})	41.24 V
Maximum current (i_{mpp})	14.55 A
Open circuit voltage (v_{oc})	48.98 V
Short circuit current (i_{sc})	15,41 A
Temperature coefficient of V_{oc}	-0.25%/ºC
Temperature coefficient of I_{sc}	0.045%/ºC

Table 2. Irradiance levels for partial shading scenarios

Scenario	Irradiance (W/m²)				
	M_1	M_2	M_3	M_4	M_5
1	1,000	1,000	1,000	1,000	1,000
2	1,000	900	800	700	600
3	1,000	850	700	550	400
4	1,000	800	600	400	200
5	950	600	350	250	150
6	950	350	200	100	50

2.2. Modeling systems

After the P-V curve variations testbeds were already simulated, MPPT was performed with four algorithms: i) P&O, ii) InC, iii) PSO, and iv) FPA. The tracking process was developed on MATLAB-Simulink R2021a software, and using a discrete fixed-step solver. The step size was set to 1×10^{-5} s, at least ten times faster than the PWM period, to accurately capture switching dynamics. The total simulation time was set to 1.5 s per scenario, sufficient to observe full convergence. Cell temperature was fixed set value at 25 °C, and sensor noise was disabled to isolate algorithmic performance.

These assumptions align with prior MPPT benchmarking studies at several works [2], [3], [26]. The MPPT controller will compute the optimal duty cycle and applies it to the boost converter to regulate PV output voltage. Converter parameters follow at Table 3; input/output capacitors $C_{\text{in}} = C_{\text{out}} = 110\ \mu$F, inductor $L = 930\ \mu$H, switching frequency $f_s = 5$ kHz, and load $R = 120\ \Omega$.

These parameter values were chosen so that the inductor current ripple remained below 10%, while output voltage ripples around its due value does not exceed 2%. This ensures stable operation during MPPT perturbations. Figure 2 depicts the system architecture testbed, configured in a standard configuration found in literature as PV → MPPT → boost converter → load, which is a common choice due to decoupling of the PV operating point from downstream loads while maintaining dynamic interactions relevant for benchmarking [3]. This setup allows for systematic testing of MPPT algorithms under multiple peak P–V characteristics brought on by partial shading.

Table 3. Parameter of the boost converter

Parameter	Value
C1	110 µF
C2	110 µF
L	930 µH
F	5 kHz
R	120 Ω

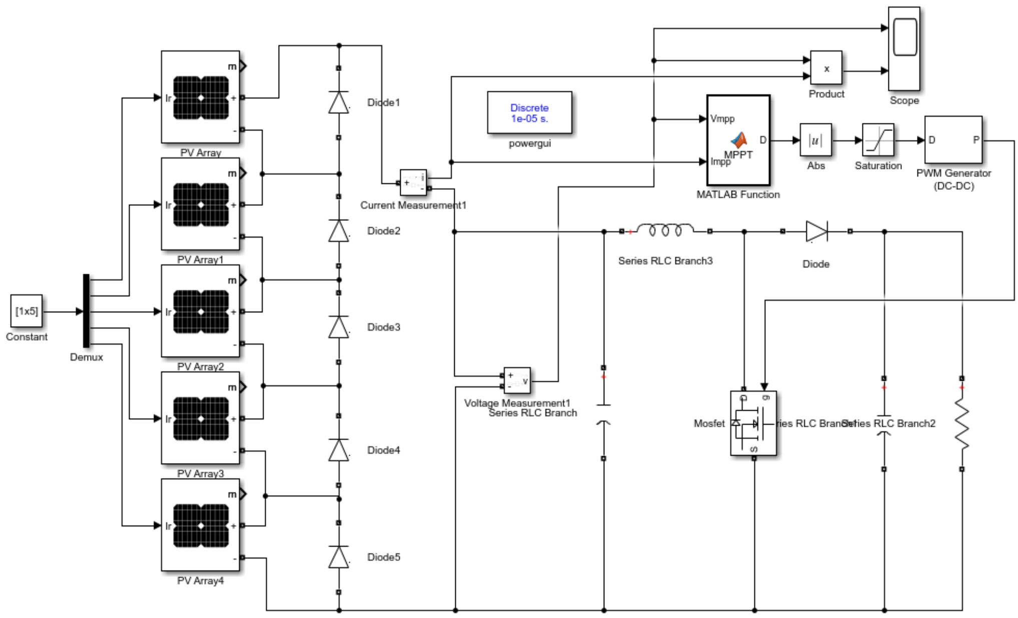

Figure 2. Modeling system

2.3. MPPT algorithms

This research using 4 MPPT algorithms for evaluated: there was i) P&O, ii) InC, iii) PSO, and iv) FPA. P&O perturbs the duty cycle and reverses direction when power decreases; a fixed step size of 0.001 was used to minimize oscillation while maintaining acceptable and convergence speed [4], [24]. InC compares $\mathrm{d}P/\mathrm{d}V$to $-I/V$ and adjusts the reference voltage dynamically; an adaptive mechanism combined with a base step size of 0.001 accelerates convergence far from the MPP [5], [27]-[29]. While PSO algorithm was configured with 5 particles, inertia weight $w = 0.5$, and acceleration coefficients $C_1 = 1.5$and $C_2 = 1.1$. for avoiding premature convergence and for the preservation of swarm diversity velocity clamping and inertia reduction were used [25], [29]. To retain global search capability over multimodal P-V landscape [10], [30], [31], FPA applied a switching probability of 0.8 and Levy flight step size of 1.5 according to previous studies that implement different variants of FPA-based MPPT algorithm [29], [30]. All algorithms that were fixed in the scenario were initialized to the same values at the beginning of each scenario and duty cycle updates coincided with the control sampling period, providing a fair comparison.

2.3.1. Perturb and observe

The P&O algorithm method is a technique used for MPPT [25]. The operation of this technique is that the voltage or current of the PV system is disturbed, and the power difference generated from disturbance will be monitored. If increasing power, the perturbation proceeds as before; if decreasing, the perturbation reverses. The process will continue until the MPP is achieved, and which is when the PV system operates at peak efficiency [32]. This relationship can be expressed mathematically as (1) and (2).

$$\Delta P = P(k) - P(k-1) \tag{1}$$

$$\Delta V = V(k) - V(k-1) \tag{2}$$

Let ΔP represent the change in power and ΔV denote the change in voltage. The flowchart of the method is depicted in Figure 3.

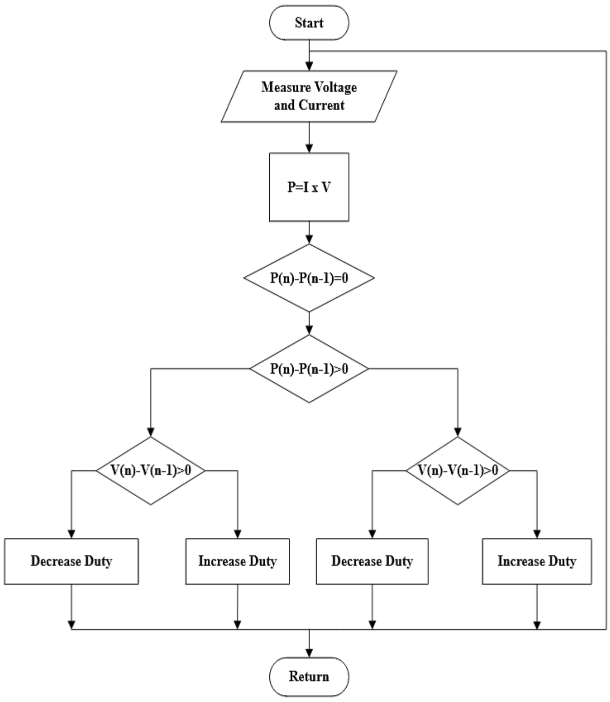

Figure 3. Flowchart of perturb and observe

2.3.2. Incremental conductance

The InC algorithm is a popular algorithm that used for optimizing the performance of solar panels by accurately determining the MPP. This algorithm operates by analyzing the slope of the power-voltage (P-V) characteristic curve of solar cells [17], [33]. The optimal operating points value, specifically the maximum power voltage (V_{MPP}) and current (I_{MPP}), are influenced by environmental factors such as irradiance and also the temperature value. The MPPT algorithm dynamically adjusts the reference voltage (V_{ref}) for ensuring the solar panel operates at their maximum power point [34]. Figure 4 describes the flowchart of incremental conductance. This relationship can be expressed mathematically as (3).

$$\frac{dP}{dV} = 0 \quad (3)$$

Let dP represent the change in power and dV denote the change in voltage. Since power P is the product of voltage and current (i.e., $P = V.I$), the above equation can be reformulated as follows:

$$\frac{dP}{dV} = \frac{d(V\times I)}{dV} = I\frac{dV}{dV} + V\frac{dI}{dV} \quad (4)$$

$$I + V\frac{dI}{dV} = 0 \quad (5)$$

$$\frac{dI}{dV} = -\frac{I}{V} \quad (6)$$

Let dI represent the current change, dV represent the voltage change, I represent the current, and V represent the voltage. The flowchart of the method is depicted in Figure 4.

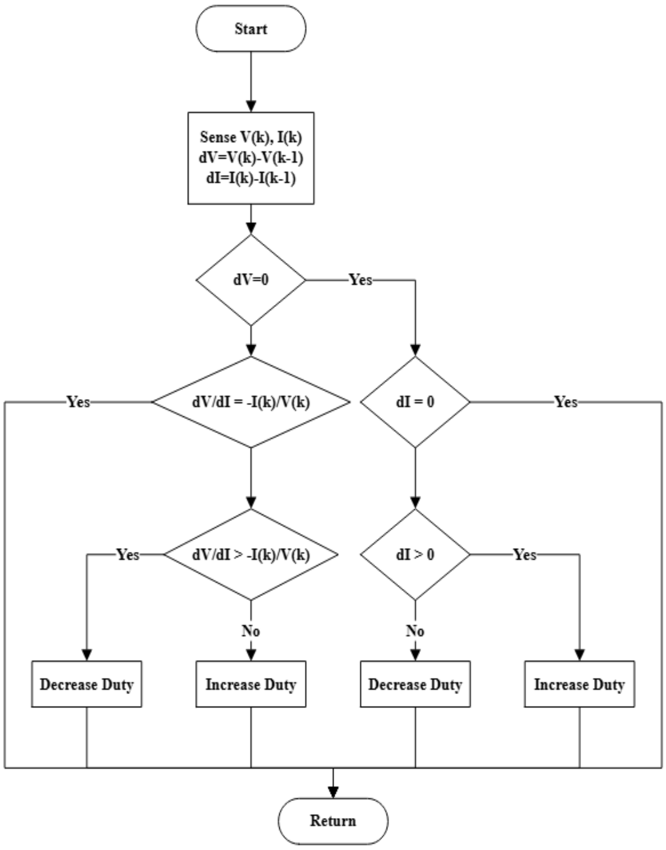

Figure 4. Flowchart of incremental conductance

2.3.3. Particle swarm optimization (PSO)

The PSO is an optimization technique that was introduced by Kennedy and Eberhart [33] based on the flocking behavior of birds in their quest for food. It is based on an algorithm that uses the flying particles in the search domain, moving by preserving memory of Pbest (individual best position) and Gbest (group best position). Essentially, devices search adjust their position depending on their own experience and those of other particles so that it gives local as well as global search ability to find better and efficient solutions [35]. Particularly, the formulae for information particles velocity update are:

$$V_i^{j+1} = W \times V_i^j + C_1\, rand1(\ \ ) \times (P_{best} - P_i^j + C_2 \times rand2(\ \ ) \times (G_{best} - P_i^j) \quad (7)$$

Let C_1 represent the cognition-only learning factor, C_2 represent the social-only learning factor, and W represent the inertia weight. The variable speed of movement of the i-th particles during the j-th iteration is denoted as V_i^j and the variable position of the i-th particle during the j-th iteration is denoted as P_i^j, The function rand1(·) generates a variable value between 0 and 1 from the first random number generator, and rand2(·) generates a variable value between 0 and 1 from the second random number generator. The term P_{best} is indicates the best position of the i-th particle, while G_{best} indicating the best position for all particles.

$$P_i^{j+1} = V_i^{j+1} + P_i^j \quad (8)$$

Where P_i^{j+1} is the position variable of the i-th updated particle during the j-th iteration, V_i^{j+1} is the velocity variable of the i-th updated particle during the j-th iteration, and P_i^j is the position variable of the i-th particle during the j-th iteration. The flowchart of the method is depicted in Figure 5.

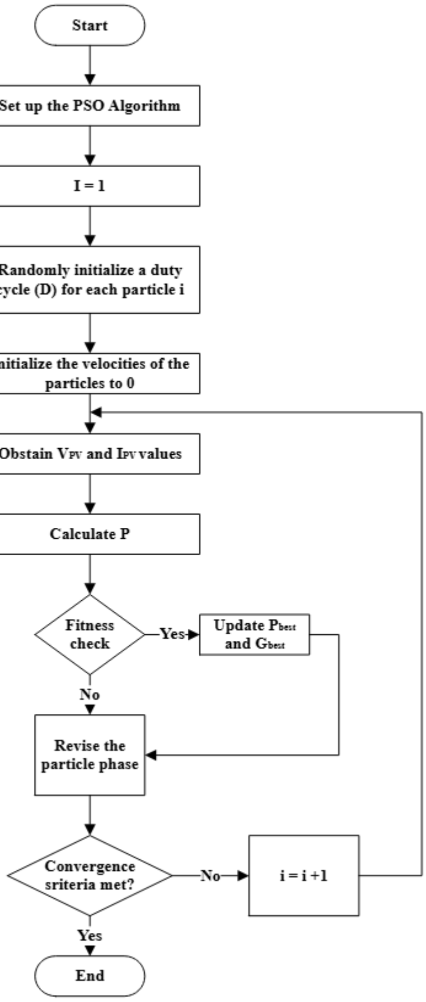

Figure 5. Flowchart of particle swarm optimization

2.3.4. Flower pollination algorithm

Pollination is divided into abiotic (self-pollination) and biotic (cross-pollination) types. Biotic pollination, performed by agents such as bees, birds, and bats, accounts for approximately 90% of the total pollination process, while abiotic pollination accounts for about 10% [36], [37]. FPA employs this principle for optimization, balancing self and cross-pollination [38] through probabilities ranging from 0 to 1. FPA implementations adhere to certain rules to mimic the pollination process effectively [39], [40].

Biotic pollination, also known as cross-pollination, involves the global movement of pollen following the pattern of Levy flight, the primary mechanism for pollen distribution. This cross-pollination process can be described by (9).

$$x_i^{k+1} = x_i^k + L + \left(gbest - x_i^k\right) \quad (9)$$

Where x_i^{k+1} is the updated solution position i at iteration k, x_i^k is solution position i at iteration k, Gbest is best solution of pollen (x_i^k), and L is the Levy factor. Levy factor plays an important role in pollen movement during the cross-pollination process [36]. Since the Levy factor affects how pollen moves, the flow of pollen movement. Through the Levy factor mechanism can be represented by (10).

$$L = \frac{\lambda\Gamma(\lambda)\sin\left(\frac{\pi\lambda}{2}\right)}{\pi}\frac{1}{S^{1+\lambda}}\left(S >> S^0 > 0\right) \quad (10)$$

The levy factor L is defined in the context of the standard gamma function $\Gamma(\lambda)$, which is valid for $S \gg S^0 > 0$, where λ represents the lambda value based on the convergence of 1.5. Abiotic pollination, also referred to as self-pollination, is a natural mechanism in which flowering plants autonomously facilitate their own pollination within the same plant, without the involvement of external agents. This pollination process is mathematically expressed in (11).

$$x_i^{k+1} = x_i^k + \varepsilon\left(x_m^k - x_j^k\right) \quad (11)$$

Where $x_j^k \; dan \; x_m^k$ are the positions of random solutions a and b from the population at iteration k, and ε is the local search representation ($\varepsilon \in (0,1)$). The flowchart of the method can be explained in Figure 6.

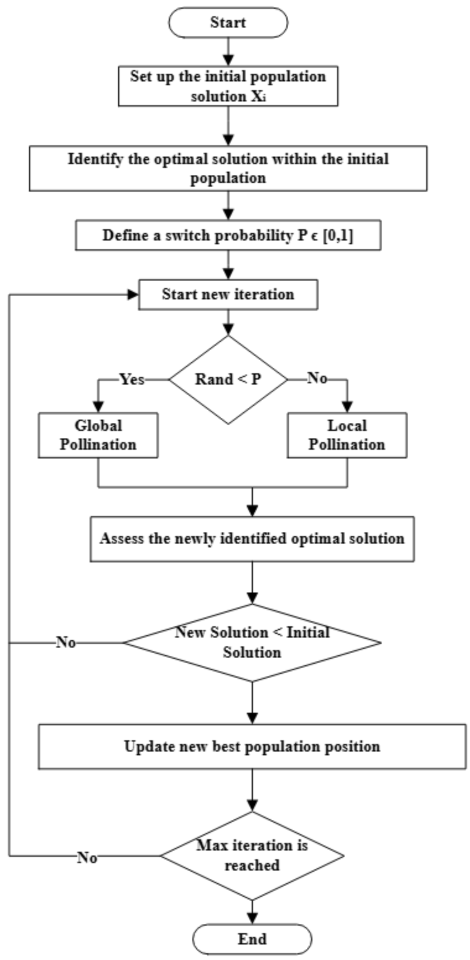

Figure 6. Flowchart of flower pollination

3. RESULTS AND DISCUSSION
3.1. Test scenario case

The P–V characteristics obtained from six tests to examine the performance of MPPT algorithm under irradiant condition are shown in Figure 7. In a single irradiance (Scenario 1), there is one type of irradiance, which creates only one MPP. Scenarios 2 to 6 mimic partial shading conditions that create multiple peaks in the P–V curve with one GMPP and four local maxima LMPPs. The GMMI position diverges between the scenarios, showing as the fifth peak for Scenario 2, and fourth peak for Scenario 3, and third peak for Scenario 4, and second peak in Scenario 5 but only first in Scenario 6. The tracking efficiency can be calculated based on the values in Table 4, which lists tracked GMPP power and voltage for all scenarios. Such scenarios offer a stringent framework for the evaluation of algorithms in terms of convergence rate, steady state, and local optimum robustness.

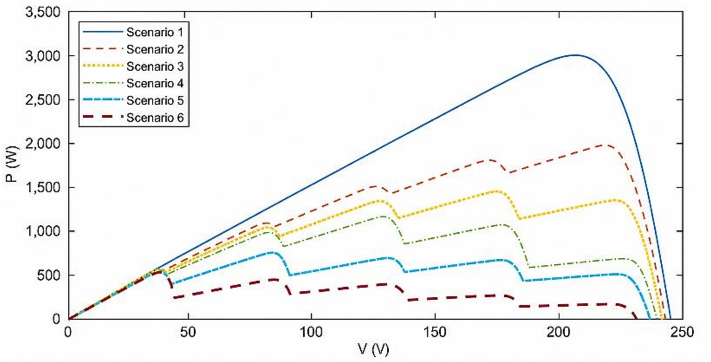

Figure 7. P-V curve under various test scenarios

Table 4. P–V curve data under different scenarios

No.	Case	Power (W)	Voltage (V)
1	Scenario 1	3,000.35	206.48
2	Scenario 2	1,976.07	218.41
3	Scenario 3	1,443.35	174.51
4	Scenario 4	1,156.63	128.77
5	Scenario 5	745.13	83.38
6	Scenario 6	525.68	38.17

3.2. Performance analysis of MPPT algorithms

The P&O, IC, PSO, and FPA algorithms are employed to track MPP under various shading conditions [16], [41]. The tracking results include power, voltage, and tracking time values, which are used to calculate the algorithm's efficiency. The resulting voltage is sent by the MPPT to the comparator, while the power and tracking time indicate the effectiveness of the algorithm in finding the MPP. The efficiency of the algorithm is calculated from the ratio of the tracked power to the actual MPP to compare the methods used.

Under uniform irradiance (Scenario 1), Figure 8 and Table 5 show that FPA and PSO achieve the highest tracked power of 2985.17 W at 209.30 V, corresponding to an efficiency of 99.494%. However, these algorithms require longer for settling times (0.753 s and 0.937 s) and exhibit significant oscillations, in power and voltage profiles. In contrast, InC and P&O converge rapidly within 0.049 s to approximately to 2977.99 W and 201.66 V with minimal oscillation, although their efficiency capability is slightly lower at 99.255%. These results indicate that InC and P&O algorithm outperform in dynamic response and stability, while FPA and PSO algorithm offer marginally better efficiency at the expense of slower convergence.

Table 5. Test results of MPPT algorithms under Scenario 1

Algorithm	Time (s)	Power (W)	Voltage (V)	Efficiency (%)
FPA	0.753	2985.170	209.295	99.494
PSO	0.937	2985.170	209.295	99.494
InC	0.049	2977.990	201.661	99.255
P&O	0.049	2977.990	201.661	99.255

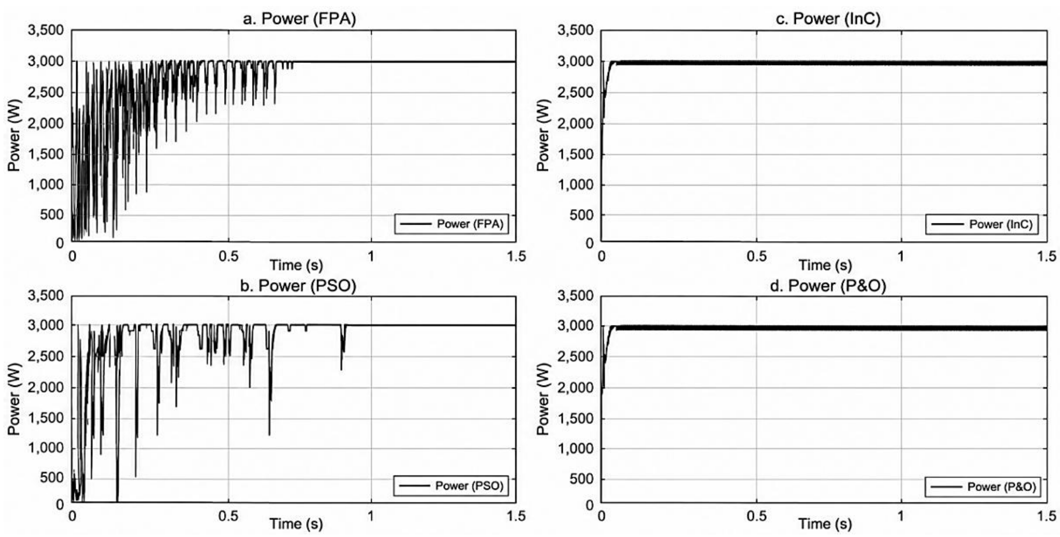

(a)

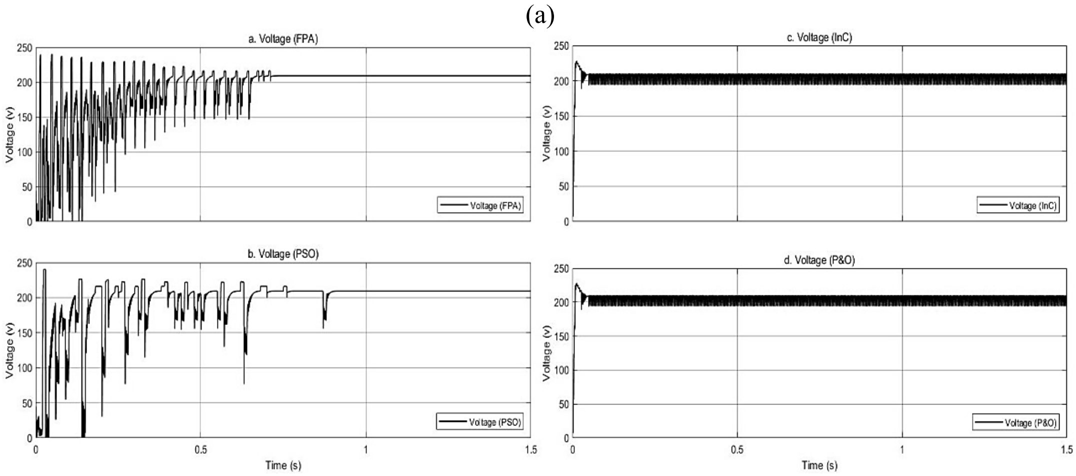

(b)

Figure 8. Comparison of MPPT performance under Scenario 1: (a) power tracking response and (b) voltage profile

In testbed for Scenario 2, introduces partial shading process with the GMPP located at the fifth peak. Figure 9 and Table 6 reveal that InC and P&O algorithm delivered superior performance, converging within 0.038 s to approximately 1965.85 W and 1965.84 W, with efficiencies value was 99.483% and 99.482%, respectively. FPA and PSO algorithm, on the other hand, require longer settling times (0.918 s and 1.381 s) and exhibit oscillatory behavior, achieving slightly lower efficiencies of 99.045%. These findings can be concluded that InC and P&O algorithm maintain high accuracy and stability under moderate complexity, whereas FPA and PSO trade speed for global search capability.

The testbed for Scenario 3, where GMPP is on the fourth peak showed that FPA and PSO algorithm have slightly higher efficiencies, 99.422% while InC and P&O achieved efficiencies of 99.356% and 99.350%, respectively as shown in Figure 10 and Table 7. On the contrary, InC and P&O converge much quicker (0.050 s and 0.051 s) with no oscillation while FPA and PSO take more than one seconds to stabilize and show substantial transient oscillations. This situation highlights the speed–accuracy trade-off between local and global search methods.

Table 6. Test results of MPPT algorithms under Scenario 2

Algorithm	Time (s)	Power (W)	Voltage (V)	Efficiency (%)
FPA	0.918	1957.200	220.291	99.045
PSO	1.381	1957.200	220.291	99.045
InC	0.038	1965.850	219.311	99.483
P&O	0.038	1965.840	219.097	99.482

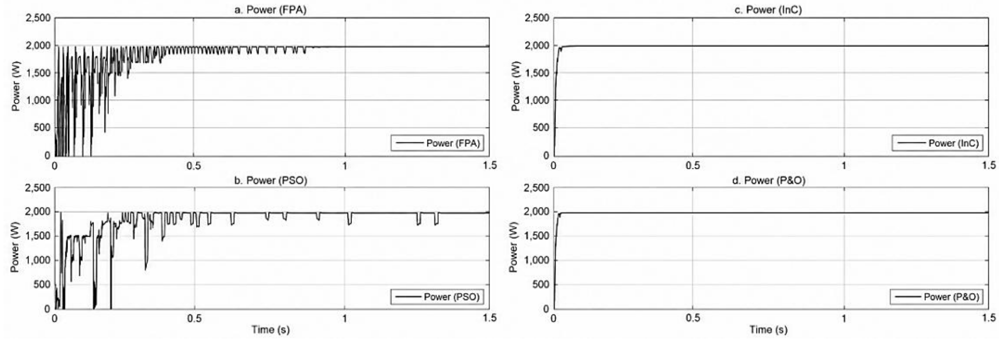

(a)

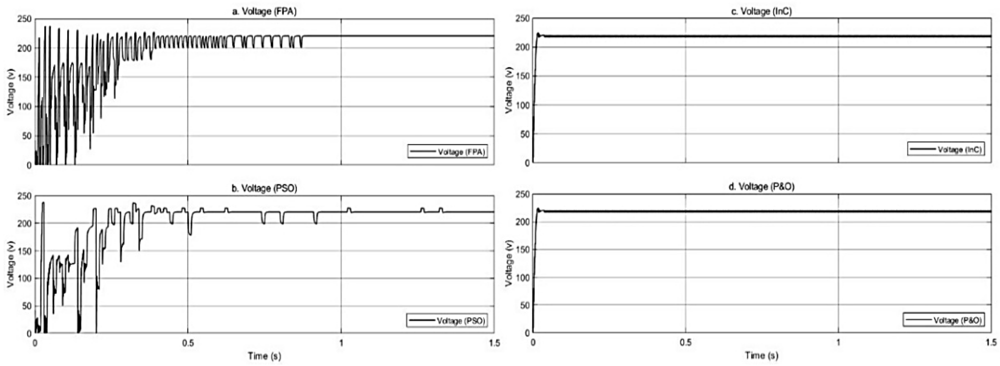

(b)

Figure 9. Comparison of MPPT performance under Scenario 2: (a) power tracking response and (b) voltage profile

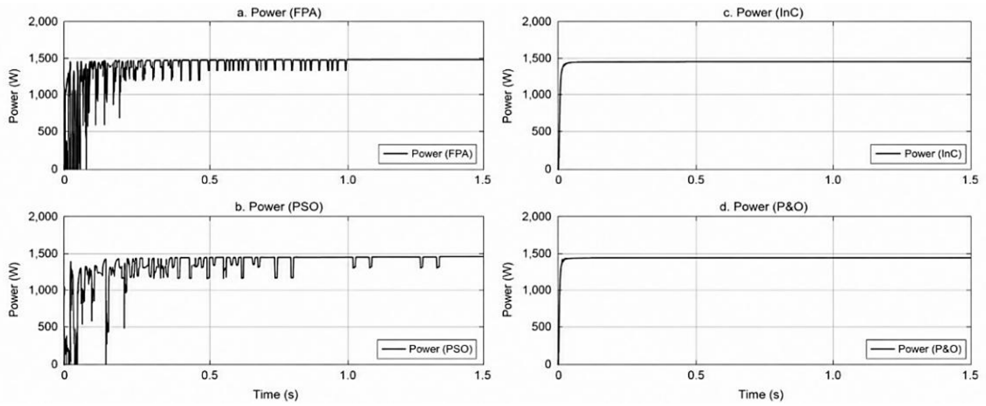

(a)

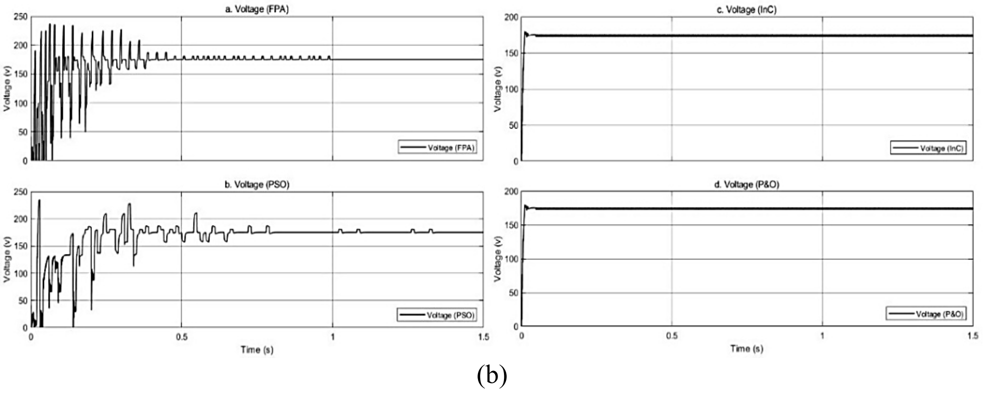

(b)

Figure 10. Comparison of MPPT performance under Scenario 3: (a) power tracking response and (b) voltage profile

Table 7. Test results of MPPT algorithms under Scenario 3

Algorithm	Time (s)	Power (W)	Voltage (V)	Efficiency (%)
FPA	1.035	1435.010	175.156	99.422
PSO	1.378	1435.010	175.156	99.422
InC	0.050	1434.050	174.809	99.356
P&O	0.051	1433.970	174.841	99.350

Scenario 4 testbed shows the more difficult case: the GMPP at third peak. As shown in Figure 11 as well as presented in Table 8 above, while FPA and PSO algorithm perfectly discover the GMPP at 1146.71W with an efficiency of 99.142%, the InC and P&O algorithm are trapped into a local maximum stabilizing at about 1061 W where an efficiency of only 91.73% is achieved. This is due to the fact that slope-based algorithms halt execution upon detection of a local peak, presuming this to be the global maximum. Meta-heuristic algorithms, on the other hand, retain global search ability but with reduced convergence rate.

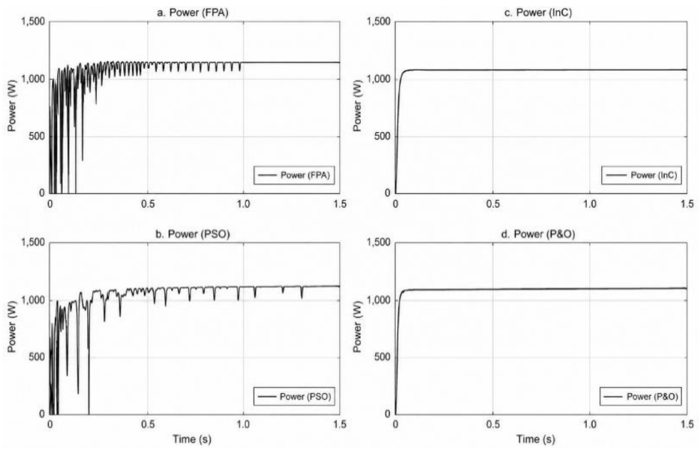

(a)

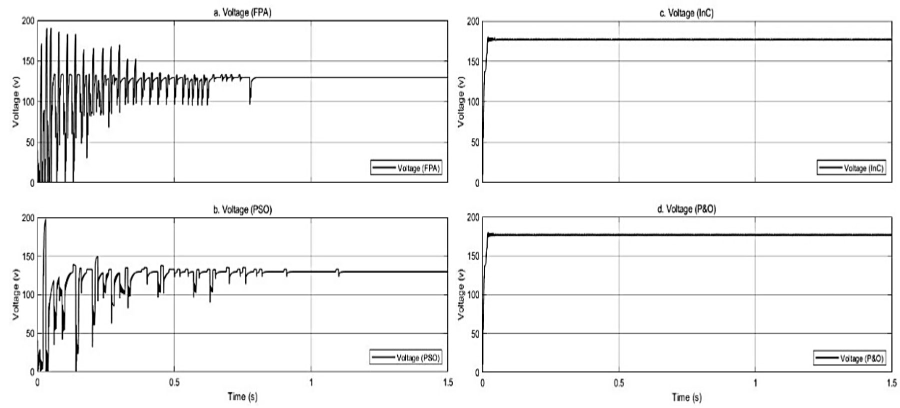

(b)

Figure 11. Comparison of MPPT performance under Scenario 4: (a) power tracking response and (b) voltage profile

Table 1. Test results of MPPT algorithms under Scenario 4

Algorithm	Time (s)	Power (W)	Voltage (v)	Efficiency (%)
FPA	0.835	1146.710	129.771	99.142
PSO	1.146	1146.710	129.771	99.142
InC	0.055	1061.030	176.196	91.735
P&O	0.048	1061.010	176.015	91.733

Testbed in Scenario 5, where the GMPP is at the second peak, all algorithms were underperformed relative to the true GMPP of 745.13 W. FPA and PSO algorithm track approximately 697.26 W (93.576% efficiency), while InC and P&O algorithm converge quickly to about 683 W (91.67%) but remain trapped at a local maximum. Figure 12 and also Table 9 suggest that parameter sensitivity and insufficient exploration hinder global convergence for meta-heuristic methods under this configuration.

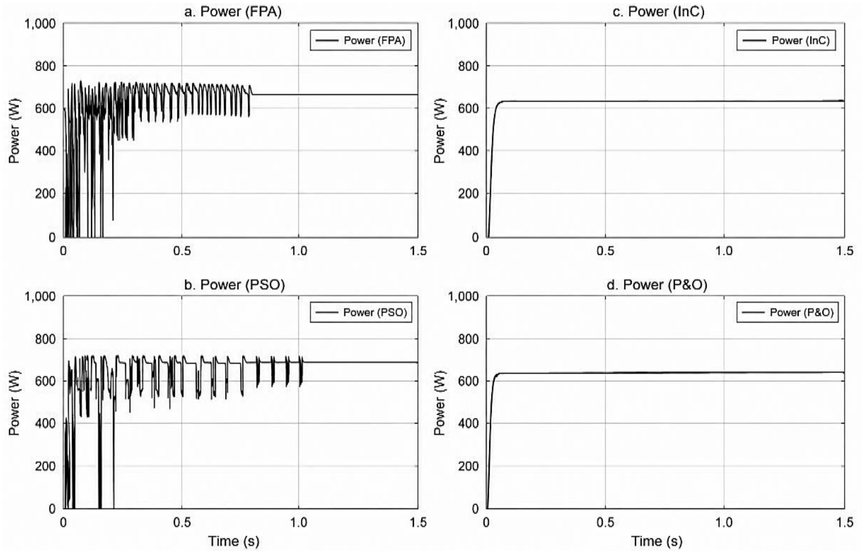

(a)

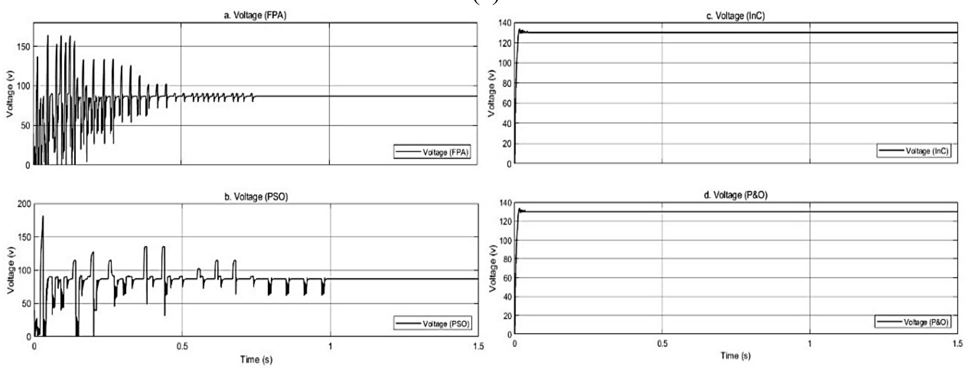

(b)

Figure 12. Comparison of MPPT performance under Scenario 5: (a) power tracking response and (b) voltage profile

Table 9. Test results of MPPT algorithms under Scenario 5

Algorithm	Time (s)	Power (W)	Voltage (v)	Efficiency (%)
FPA	0.771	697.264	86.815	93.576
PSO	1.008	697.264	86.815	93.576
InC	0.064	683.050	130.162	91.669
P&O	0.069	683.040	130.162	91.667

Finally, testbed for Scenario 6 places the GMPP at the first peak, representing the most complex shading pattern. Figures 13 and also Table 10 show that FPA algorithm achieves near-perfect tracking at 524.67 W (99.807% efficiency) after 0.802 s, while PSO, InC, and P&O algorithm converge faster but stabilize at approximately 439.52 W (83.61%), confirming entrapment at a local maximum. These results highlight the robustness of FPA algorithm in global optimization and the vulnerability of PSO to premature convergence when particle diversity collapses.

The comparative analysis shows that for all scenarios the slope-based algorithms such as InC and P&O never achieve the GMPP when it is located at the last peak of the P–V curve which occurs in Scenarios 4, 5, and 6. Its derivative-based decision-making leads to their fast convergence, but stops at the local maxima. The PSO performs well in moderately complex conditions, but poorly on highly multimodal profiles, especially when the GMPP is placed at peak number five due to premature convergence given by particle clustering. Conversely, under all scenarios examined, the FPA always identifies the GMPP, offering convincing evidence of its superior global search ability than due to prolonged settling time and intermediate oscillation. The robustness of FPA was higher compared to the five other algorithms because they faced a LMPP entrapment in Scenario 6, and their average efficiencies dropped by 16.2% even though P&O

performed with efficiency equal to 83.3%, while PSO worked on its best condition at this time with performance declining such as well, where FPA gave its highest-efficiency at Scenario 6 (99.80%). Therefore, these research results highlight the necessity for hybrid MPPT schemes that can strike a balance between fast local convergence and global optimization to provide optimum steady performance of PV under drastic shading conditions.

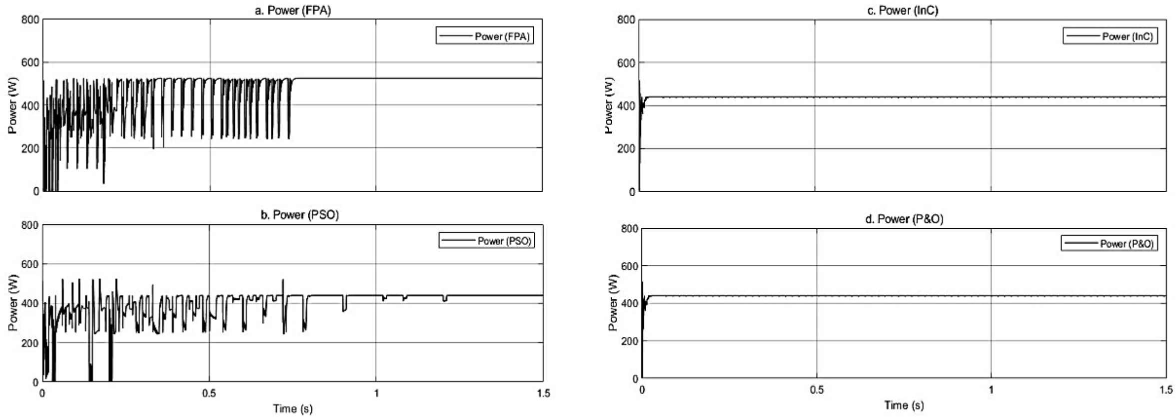

(a)

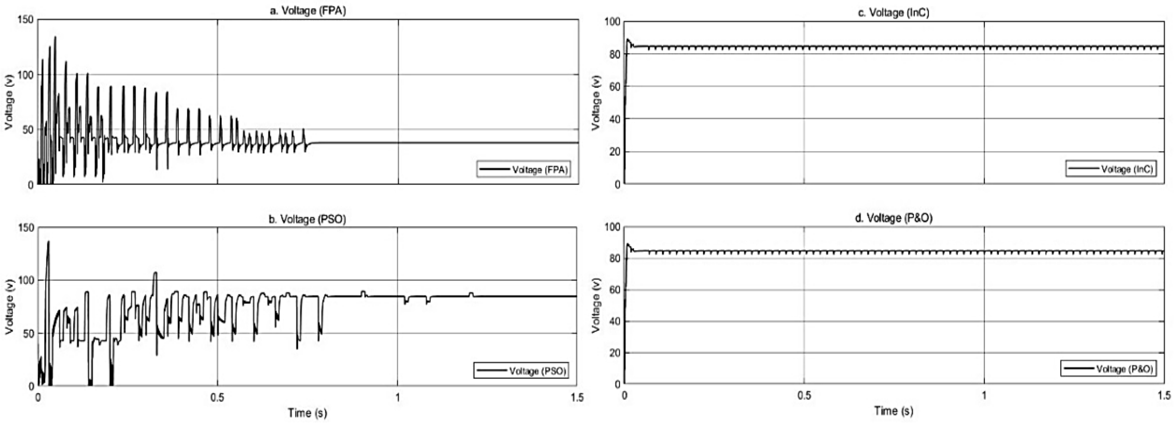

(b)

Figure 13. Comparison of MPPT performance under Scenario 6: (a) power tracking response and (b) voltage profile

Table 10. Test results of MPPT algorithms under Scenario 6

Algorithm	Time (s)	Power (W)	Voltage (v)	Efficiency (%)
FPA	0.802	524.665	38.073	99.807
PSO	1.257	439.517	84.573	83.609
InC	0.049	439.529	84.557	83.612
P&O	0.049	439.528	84.557	83.611

4. CONCLUSION

This research provides a systematic comparative evaluation algorithm of i) P&O, ii) InC, iii) PSO, and iv) FPA algorithms across six irradiance scenarios testbed, ranging from uniform to severe partial shading. The results concluded that a clear trade-off between tracking speed and global optimization capability. Under uniform and low-complexity conditions (Scenarios 1–3), slope-based algorithms (P&O and InC) outperform metaheuristics in terms of dynamic response, achieving convergence in less than 0.051 s with high efficiency (>99%). However, these algorithms consistently fail in multimodal P–V landscapes (shown on Scenarios 4–6), becoming trapped in local maxima with efficiency dropping as low as 83.61%. Among the metaheuristic approaches, PSO algorithm shows vulnerability to premature convergence in highly complex scenarios, particularly when the GMPP is located at the first peak.

In contrast, FPA algorithm demonstrates superior robustness performance, consistently identifying the GMPP across all test cases with a peak tracking efficiency of at 99.81% in the most challenging scenario. Despite its accuracy, FPA algorithm requires a significantly longer settling time (averaging 0.8 s to 1.0 s) and exhibits transient oscillations during the global search phase. These findings of research suggest that while FPA algorithm is highly reliable for complex shading, its implementation requires careful consideration of computational overhead and sampling rates in real-time embedded systems application. Future research will focus on developing hybrid frameworks that combine the rapid local convergence of InC with the global search power of FPA to minimize energy loss during the tracking transition.

FUNDING INFORMATION

The authors would like to express their sincere gratitude to all contributors whose valuable input and collaboration made this work possible. Special thanks are also extended to LPPM University of Lampung for providing continuous support, resources, and an enabling academic environment.

AUTHOR CONTRIBUTIONS STATEMENT

This journal uses the Contributor Roles Taxonomy (CRediT) to recognize individual author contributions, reduce authorship disputes, and facilitate collaboration.

Name of Author	C	M	So	Va	Fo	I	R	D	O	E	Vi	Su	P	Fu
Dikpride Despa	✓	✓		✓	✓	✓	✓	✓	✓	✓		✓	✓	✓
Gigih Forda Nama		✓	✓	✓	✓	✓		✓	✓	✓	✓	✓	✓	
Zulmiftahul Huda		✓	✓	✓	✓		✓	✓		✓	✓		✓	
Stefanus Debiarto		✓	✓		✓		✓		✓	✓	✓		✓	
Marudut Sagala														

C : **C**onceptualization
M : **M**ethodology
So : **So**ftware
Va : **Va**lidation
Fo : **Fo**rmal analysis
I : **I**nvestigation
R : **R**esources
D : **D**ata Curation
O : Writing - **O**riginal Draft
E : Writing - Review & **E**diting
Vi : **Vi**sualization
Su : **Su**pervision
P : **P**roject administration
Fu : **Fu**nding acquisition

CONFLICT OF INTEREST STATEMENT

Authors state no conflict of interest.

DATA AVAILABILITY

The data presented in this paper is newly obtained during the research and is not yet publicly available. Data is contained within the article.

REFERENCES

[1] A. Luque and S. Hegedus, "Bulk crystal growth and wafering for PV," in *Handbook of Photovoltaic Science and Engineering*, Wiley, 2003, pp. 205–254. doi: 10.1002/0470014008.ch6.

[2] M. Y. Worku *et al.*, "A comprehensive review of recent maximum power point tracking techniques for photovoltaic systems under partial shading," *Sustainability (Switzerland)*, vol. 15, no. 14, 2023, doi: 10.3390/su151411132.

[3] M. A. G. De Brito, L. Galotto, L. P. Sampaio, G. De Azevedo Melo, and C. A. Canesin, "Evaluation of the main MPPT techniques for photovoltaic applications," *IEEE Transactions on Industrial Electronics*, vol. 60, no. 3, pp. 1156–1167, 2013, doi: 10.1109/TIE.2012.2198036.

[4] C. I William and R. R, "Comparative study of P&O and InC MPPT algorithms," *American Journal of Engineering Research (AJER)*, vol. 02, no. 12, pp. 402–408, 2013.

[5] I. V. Banu, R. Beniuga, and M. Istrate, "Comparative analysis of the perturb-and-observe and incremental conductance MPPT methods," *2013 - 8th International Symposium on Advanced Topics in Electrical Engineering, ATEE 2013*, 2013, doi: 10.1109/ATEE.2013.6563483.

[6] K. S. Tey, S. Mekhilef, H.-T. Yang, and M.-K. Chuang, "A differential evolution based MPPT method for photovoltaic modules under partial shading conditions," *International Journal of Photoenergy*, vol. 2014, pp. 1–10, 2014, doi: 10.1155/2014/945906.

[7] S. B. R. Chowdhury, A. Mukherjee, and P. K. Gayen, "Maximum power point tracking of photovoltaic system by perturb & observe and incremental conductance methods under normal and partial shading conditions," in *2021 Innovations in Energy Management and Renewable Resources (52042)*, Feb. 2021, pp. 1–6, doi: 10.1109/IEMRE52042.2021.9386964.

[8] L. M. Satapathy, A. Harshita, M. Saif, P. K. Dalai, and S. Jena, "Comparative analysis of boost and buck-boost converter in photovoltaic power system under varying irradiance using MPPT," *Proceedings of the International Conference on Inventive Communication and Computational Technologies, ICICCT 2018*, pp. 1828–1833, 2018, doi: 10.1109/ICICCT.2018.8473222.
[9] A. Ibrahim *et al.*, "PV maximum power-point tracking using modified particle swarm optimization under partial shading conditions," *Chinese Journal of Electrical Engineering*, vol. 6, no. 4, pp. 106–121, Dec. 2020, doi: 10.23919/CJEE.2020.000035.
[10] J. Prasanth Ram and N. Rajasekar, "A novel flower pollination based global maximum power point method for solar maximum power point tracking," *IEEE Transactions on Power Electronics*, vol. 32, no. 11, pp. 8486–8499, 2017, doi: 10.1109/TPEL.2016.2645449.
[11] N. M. Elbehairy, R. A. Swief, A. M. Abdin, and T. S. Abdelsalam, "Maximum power point tracking for a stand alone PV system under shading conditions using flower pollination algorithm," in *2019 21st International Middle East Power Systems Conference (MEPCON)*, Dec. 2019, pp. 840–845, doi: 10.1109/MEPCON47431.2019.9008230.
[12] A. Chellakhi, S. El Beid, Y. Abouelmahjoub, and H. Doubabi, "An enhanced incremental conductance MPPT Approach for PV power optimization: a simulation and experimental study," *Arabian Journal for Science and Engineering*, vol. 49, no. 12, pp. 16045–16064, 2024, doi: 10.1007/s13369-024-08804-1.
[13] K. Ishaque, Z. Salam, and G. Lauss, "The performance of perturb and observe and incremental conductance maximum power point tracking method under dynamic weather conditions," *Applied Energy*, vol. 119, pp. 228–236, Apr. 2014, doi: 10.1016/j.apenergy.2013.12.054.
[14] N. Pamuk, "Performance analysis of different optimization algorithms for MPPT control techniques under complex partial shading conditions in PV systems," *Energies*, vol. 16, no. 8, p. 3358, 2023, doi: 10.3390/en16083358.
[15] H. Rezk *et al.*, "A novel statistical performance evaluation of most modern optimization-based global MPPT techniques for partially shaded PV system," *Renewable and Sustainable Energy Reviews*, vol. 115, 2019, doi: 10.1016/j.rser.2019.109372.
[16] J. Gosumbonggot and G. Fujita, "Partial shading detection and global maximum power point tracking algorithm for photovoltaic with the variation of irradiation and temperature," *Energies*, vol. 12, no. 2, 2019, doi: 10.3390/en12020202.
[17] M. Ben Aicha, N. Hacene, and A. Teta, "Comparative study of P & O and PSO-based MPPT algorithms for PV systems under partial shading conditions Comparative study of P & O and PSO-based MPPT algorithms for PV systems under partial shading conditions," *ResearchGate*, no. June, pp. 1–9, 2025.
[18] G. M. S. Martines, M. A. G. De Brito, E. A. Batista, R. B. Godoy, and T. H. A. Mateus, "Sensorless MPPT algorithms for PV systems in partially shaded scenarios," *Eletrônica de Potência*, vol. 29, p. e202452, 2024, doi: 10.18618/rep.e202452.
[19] A. A. Kamil, M. S. Nasr, and S. Alwash, "Maximum power point tracking method for photovoltaic system based on enhanced particle swarm optimization algorithm under partial shading condition," *International Journal of Intelligent Engineering and Systems*, vol. 13, no. 6, pp. 241–254, 2020, doi: 10.22266/ijies2020.1231.22.
[20] S. Liu *et al.*, "A parameter estimation of photovoltaic models using a boosting flower pollination algorithm," *Sensors*, vol. 23, no. 19, p. 8324, Oct. 2023, doi: 10.3390/s23198324.
[21] M. Shafiul, S. Datta, S. Sara, and N.-E.-A. Tabassum, "Flower pollination algorithm with linearly varying exploration: a novel approach for continuous function optimization problem," *Communications on Applied Electronics*, vol. 7, no. 16, pp. 51–56, May 2018, doi: 10.5120/cae2018652768.
[22] B. U. D. Abdullah, S. L. Dhar, S. P. Jaiswal, M. M. Gulzar, M. Alqahtani, and M. Khalid, "Hybrid MPPT control using hybrid pelican optimization algorithm with perturb and observe for PV connected grid," *Frontiers in Energy Research*, vol. 12, Jan. 2025, doi: 10.3389/fenrg.2024.1505419.
[23] Jahid, M. Ehtesham, S. Kirmani, and Manaullah, "Application of flower pollination algorithm and its comparative analysis for MPPT of solar panels under partial shading conditions," *Journal of The Institution of Engineers (India): Series B*, vol. 106, no. 6, pp. 1829–1842, 2025, doi: 10.1007/s40031-025-01197-1.
[24] A. Saberi, M. Niroomand, and B. M. Dehkordi, "An improved P&O based MPPT for PV systems with reduced steady-state oscillation," *International Journal of Energy Research*, vol. 2023, 2023, doi: 10.1155/2023/4694583.
[25] M. A. M. Villalobos, J. E. S. Martínez, D. J. Rincon, Y. Rodríguez, and L. T. Leon, "Comparative analysis of MPPT algorithms for PV systems under partial shading conditions," *Simposio Internacional sobre la Calidad de la Energía Eléctrica (SICEL)*, vol. 10, 2021.
[26] A. E. Mohammed, Z. Bashar, and J. A. David, "Assessment of perturb and observe MPPT algorithm implementation techniques for PV pumping applications," *IEEE Transactions on Sustainable Energy,* vol. 3, no. 1, pp. 21–33, 2011.
[27] K. Sabri, O. El Maguiri, and A. Farchi, "Comparative study of different MPPT algorithms for photovoltaic systems under partial shading conditions," *Proceedings of 2021 9th International Renewable and Sustainable Energy Conference, IRSEC 2021*, 2021, doi: 10.1109/IRSEC53969.2021.9741164.
[28] M. Agdam, A. Asbayou, M. Elyaqouti, A. Ihlal, and K. Assalaou, "MPPT of PV system under partial shading conditions based on bio-inspired swarm intelligence technique," in *E3S Web of Conferences*, 2021, vol. 297, doi: 10.1051/e3sconf/202129701051.
[29] Z. Erdem, "A review of MPPT algorithms for partial shading conditions," *Acta Physica Polonica A*, vol. 132, no. 3, pp. 1128–1133, 2017, doi: 10.12693/APhysPolA.132.1128.
[30] D. Yousri, T. S. Babu, D. Allam, V. K. Ramachandaramurthy, and M. B. Etiba, "A novel chaotic flower pollination algorithm for global maximum power point tracking for photovoltaic system under partial shading conditions," *IEEE Access*, vol. 7, pp. 121432–121445, 2019, doi: 10.1109/ACCESS.2019.2937600.
[31] R. S. Ponugoti, "Comparative study of P&O and incremental conductance MPPT algorithms for photovoltaic system," *International Journal of Innovations in Engineering and Technology (IJIET)*, vol. 23, pp. 200–206, 2016.
[32] A. Sadick, "Maximum power point tracking simulation for photovoltaic systems using perturb and observe algorithm," in *Solar Radiation - Enabling Technologies, Recent Innovations, and Advancements for Energy Transition*, IntechOpen, 2023, doi: 10.5772/intechopen.111632.
[33] J. Kennedy and R. Eberhart, "Particle swarm optimization," in *Proceedings of ICNN'95 - International Conference on Neural Networks*, 1995, vol. 4, pp. 1942–1948. doi: 10.1109/ICNN.1995.488968.
[34] D. Sera, L. Mathe, T. Kerekes, S. V. Spataru, and R. Teodorescu, "On the perturb-and-observe and incremental conductance MPPT methods for PV systems," *IEEE Journal of Photovoltaics*, vol. 3, no. 3, pp. 1070–1078, Jul. 2013, doi: 10.1109/JPHOTOV.2013.2261118.
[35] C. Gonzalez-Castano, C. Restrepo, S. Kouro, and J. Rodriguez, "MPPT algorithm based on artificial bee colony for PV system," *IEEE Access*, vol. 9, pp. 43121–43133, 2021, doi: 10.1109/ACCESS.2021.3066281.
[36] L. Shang, W. Zhu, P. Li, and H. Guo, "Maximum power point tracking of PV system under partial shading conditions through flower pollination algorithm," *Protection and Control of Modern Power Systems*, vol. 3, no. 1, p. 38, Dec. 2018, doi: 10.1186/s41601-018-0111-3.

[37] F. D. Murdianto, A. S. L. Hermawan, A. R. Nansur, and R. E. Setiawan, "Comparison method of flower pollination algorithm, modified particle swarm optimization and perturb & observe in MPPT coupled inductor SEPIC converter on DC microgrid isolated system," in *2017 International Conference on Advanced Mechatronics, Intelligent Manufacture, and Industrial Automation (ICAMIMIA)*, Oct. 2017, pp. 291–296, doi: 10.1109/ICAMIMIA.2017.8387604.
[38] M. Abdel-Basset and L. A. Shawky, "Flower pollination algorithm: a comprehensive review," *Artificial Intelligence Review*, vol. 52, no. 4, pp. 2533–2557, Dec. 2019, doi: 10.1007/s10462-018-9624-4.
[39] T.-T. Nguyen, J.-S. Pan, and T.-K. Dao, "An improved flower pollination algorithm for optimizing layouts of nodes in wireless sensor network," *IEEE Access*, vol. 7, pp. 75985–75998, 2019, doi: 10.1109/ACCESS.2019.2921721.
[40] B. Kumar and A. Kumar, "A novel adaptive flower pollination algorithm for maximum power tracking of photovoltaic systems under dynamic shading conditions," *Iranian Journal of Science and Technology, Transactions of Electrical Engineering*, vol. 48, no. 2, pp. 859–875, Jun. 2024, doi: 10.1007/s40998-024-00696-z.
[41] R. Sen, A. Garg, and A. Singh, "Modeling of PV array using P&O algorithm in boost converter," *2017 International Conference on Computing and Communication Technologies for Smart Nation, IC3TSN 2017*, 2017, pp. 231–236, doi: 10.1109/IC3TSN.2017.8284482.

BIOGRAPHIES OF AUTHORS

Dikpride Despa is a lecturer at the Department of Electrical Engineering, Faculty of Engineering, University of Lampung, Indonesia. Born in Pariaman, West Sumatra, she holds a master's degree from Institut Teknologi Sepuluh Nopember (1997) and a doctorate from Kyushu Institute of Technology, Japan (2012). Her research interests include electronics, power systems, renewable energy, energy audit, and internet of things (IoT). She can be contacted at email: despa@eng.unila.ac.id.

Gigih Forda Nama is a researcher at the Department of Informatics, University of Lampung, specializing in computer networking, cloud computing, internet of things (IoT), data mining, service-oriented architecture (SOA), enterprise architecture, IT risk management, and information technology. He earned his master's degree in information technology from Universitas Indonesia and completed his bachelor's in electrical engineering at University of Lampung. He can be contacted at email: gigih@eng.unila.ac.id.

Zulmiftahul Huda is a lecturer in the Department of Electrical Engineering at the Faculty of Engineering, University of Lampung, Indonesia, specializing in undergraduate-level electrical engineering. His academic credentials include a Bachelor of Engineering and a Master of Engineering, and he is actively involved in education and research at University of Lampung. He can be contacted at email: zulmiftah.huda@eng.unila.ac.id.

Stefanus Debiarto Marudut Sagala received the B.S. degree in electrical engineering from Lampung University, Bandar Lampung, Indonesia, in 2024. His research interests include the implementation of swarm-based metaheuristic algorithms for maximum power point tracking (MPPT) in renewable energy systems. He can be contacted at email: stefanus9799@gmail.com.